

OPTICAL TOMOGRAPHY FOR MEASURING DOSE DISTRIBUTION IN RADIATION THERAPY

by

Matti KAUPPINEN¹, **Esko ALASAARELA**^{2*}, **Antero KOIVULA**³, and **Sini ROUHIAINEN**³

¹ Detection Technology, Inc., Ii, Finland

² Department of Electrical Engineering, University of Oulu, Oulu, Finland

³ Department of Radiotherapy, Oulu University Hospital and Medical Research Center, Oulu, Finland

Scientific paper

DOI: 10.2298/NTRP1403213K

The dosimetry is used to verify the dose magnitude with artificial samples (phantoms) before giving the planned radiation therapy to the patient. Typically, dose distribution is measured only in a single point or on a two-dimensional matrix plane. New techniques of radiation therapy ensure more detailed planning of radiation dose distribution which will lead to the need of measuring the radiation dose distribution three-dimensionally. The gel dosimetry is used to indicate and determine the ionizing radiation three-dimensionally. The radiation causes changes in chemical properties of the gel. The radiation dose distribution is defined by measuring the chemical changes. A conventional method is the magnetic resonance imaging and a new possibility is optical computed tomography (optical-CT). The optical-CT is much cheaper and more practical than magnetic resonance imaging. In this project, an optical-CT based method device was built by aiming at low material costs and a simple realization. The constructed device applies the charge coupled device camera and fluorescent lamp technologies. The test results show that the opacity level of the radiated gel can be measured accurately enough. The imaging accuracy is restricted by the optical distortion, *e. g.* vignetting, of the lenses, the distortion of a fluorescent lamp as the light source and a noisy measuring environment.

Index terms: gel dosimetry, measuring opacity, optical-CT, tomography, verification of radiation therapy

INTRODUCTION

Intensity modulated radiation therapy (IMRT) is based on the use of an accurate three-dimensional distribution of the radiation dose. This leads to a need for a higher quality control for the determination of the dose distribution [1]. This is usually done by radiating a gel phantom first and determining the chemical changes which can be measured either by magnetic or optical methods. The gel dosimetry has traditionally been based on magnetic resonance imaging (MRI), but optical computed tomography (optical-CT) has come to be an alternative [2]. There is a clear need for a reliable, inexpensive and accurate measuring device for determining the chemical changes of the gel. It would remarkably widen the use of gel dosimetry.

The optical-CT utilizes the changes of the opacity of the gel due to the radiated dose. It is important that the opacity changes are linear or at least deterministic for a mathematical calculation of the radiated dose of the opacity change.

This study focuses on problems of applying an optical-CT to determine the dose distribution. A special objective is to analyze the optical properties of a MAGAT gel, which has in previous studies been found to be a good method to determine the magnetic changes [3-5].

The basic principle of the optical computed tomography is the same as with the X-ray computed tomography. The object is illuminated with a light source from one side and the transposed energy is defined by a linear array of detectors on the opposite side of the object. The object (or the transmitter receiver mechanism) is rotated incrementally, little by little, and the illumination is done from each angle of view. The cross-sectional image opacity of the object can then be reconstructed from the measured data of the transposed light energy.

In this study, the reconstruction process is based on an inverse radon transform [6], although iterative algorithms could have given even better quality of tomography images. The radon transform is mathematically

* Corresponding author; e-mail: esko.alasaarela@ee.ouli.fi

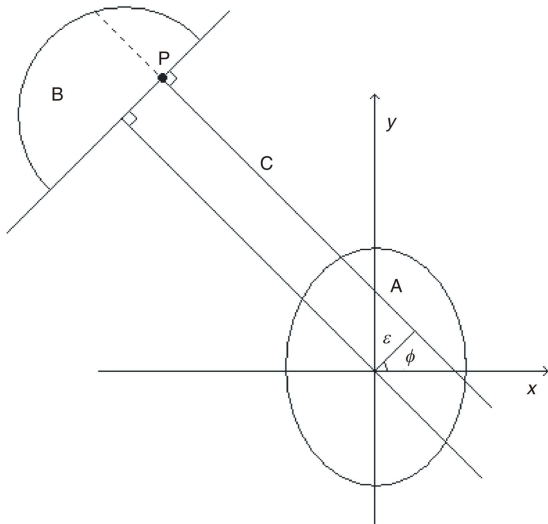


Figure 1. Co-ordinate system and variables of the radon transform

$$p(\xi, \phi) = \int_{-\infty}^{\infty} \int_{-\infty}^{\infty} f(x, y) \delta(x \cos \phi - y \sin \phi - \xi) dx dy \quad (1)$$

where δ is the unit impulse function, x and y – the co-ordinates in the object space, ξ – the distance of the beam from the origin, and ϕ – the projection angle [7]. The ξ and ϕ are the so called sinogram co-ordinates. The radon transform utilises transposed projections. The co-ordinate system and variables are defined in fig. 1.

A is the distribution in the object and the radon transform gives the projections B. The point P is a single point of the projection with its value. Equation 1 gives the values of the projection B from two dimensional data of the object A.

The inverse radon transform defines the cross-sectional tomography image points of the object from the projection data. Mathematically it is

$$f_{BP}(x, y) = \int_0^{\pi} p(x \cos \phi - y \sin \phi, \phi) d\phi \quad (2)$$

where the integration from 0 to π is enough because the integration from π to 2π gives the same information. Practically, the tomography image which is calculated directly by the inverse radon transform is inaccurate, due to the finite sampling rate of the measurement array [8]. The finite number of sensors and projection angles leads to a finite number of slice data. The frequency domain cannot be filled completely, and far from the origin, the interpolate error grows. This is called the $1/r$ inaccuracy [9]. In the tomography image, the error grows as a function of spatial frequency.

A filtered back projection method has been developed to minimize this error. A sinogram calculated from the projections is filtered by a focusing high pass filter before the back projection. The filter properties have to be selected case-specifically. The filtered back projection happens in two phases. First, the sinogram

is filtered directly by convolution or transformed into the frequency domain by a fast Fourier transform, multiplied by the filter function and returned back by an inverse Fourier transform. Second, the back projection is finalized by summing the dragged projections up, maintaining their original angles. [10]

The refraction on material boundaries affects the reliability of the results in optical measurements. The refraction phenomenon complies with Snell's law

$$n_1 \sin \phi_1 = n_2 \sin \phi_2 \quad (3)$$

where sub-indices 1 and 2 refer to two different materials, n is the refraction coefficient and ϕ is the angle between the beam and the boundary surface [11]. The refraction can be minimized by using perpendicular surfaces and materials with similar refraction coefficients. Figure 2 presents the refraction of light beams on the boundaries between gel, the gel container and the surrounding matching material.

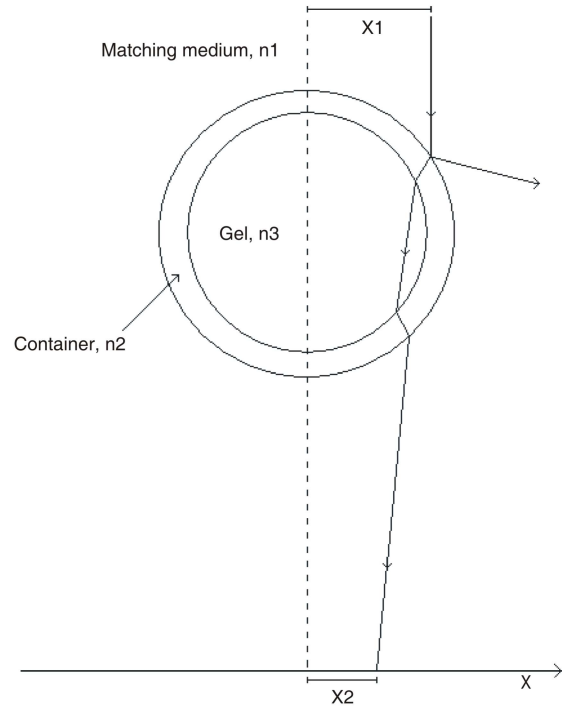


Figure 2. Refraction of light on boundaries

CONSTRUCTED MEASUREMENT TECHNIQUE

Two main techniques have been used in optical tomography. One is based on a coherent laser beam [12-15] and another on a CCD cell technique proposed originally by Wolodzko [16-22]. The latter utilizes the incoherent light and a CCD camera (fig. 3).

In this study, the CCD camera technique was applied. The light source was a fluorescent lamp with a diffuser window. The gel was set on a turntable and

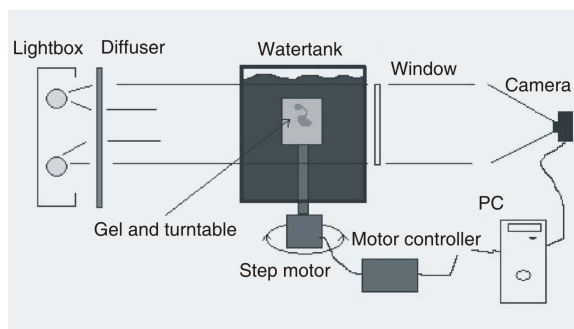


Figure 3. Principle of an optical-CT based on CCD camera

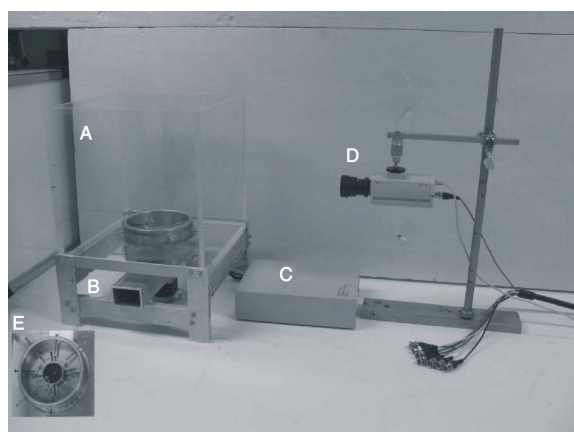


Figure 4. The constructed installation: A – the water tank, B – the basement of the water tank with the step motor and turntable, C – the step motor driver, D – the CCD camera with a stand, and E a mechanism for fixation of gels

immersed in an acrylic water tank. The turntable was rotated by a hybrid step motor, which was driven by an Applied Motion Products 3540i driver. The step motor driver was controlled by a PC. The CCD camera was a Philips LTC 0330/51 with a Maxtor Meteor II frame grabber and software. Two different objectives were tested: the Philips LTC 3361/20 2.8-6 mm 1:1.2 and the Canon TV-Zoom lens J6x11 11-70 mm 1:1.4. The water was used as a matching medium to minimize the refraction problems (fig. 4).

A user interface of the developed software can be seen in fig. 5. It controls both the projection angle setting and the image capturing. The projection images are stored as 8 bit TIFF files.

Another software was developed for the back projection process. A filtered algorithm was adopted with two alternative filter functions: the Shepp-Logan or Ram-Lak filters [23, 24].

The direct expenses of the optical-CT device were far below 3000 €, which was much less than using the MRI. Also, the functional expenses are lower, with a faster performance. All measurements were done in a room temperature of 22 degrees centigrade

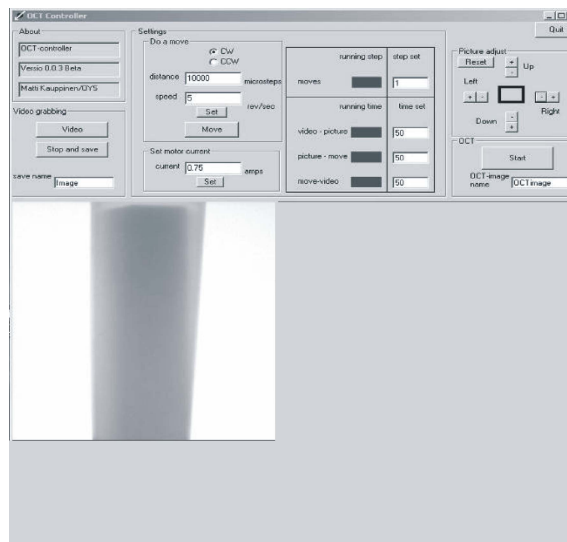


Figure 5. User interface of the constructed optical tomography installation. A projection image of a gel radiated with a square field can be seen in the display

and no temperature control was used. Also no study on dependency between the light source wavelength and the temperature was included because of the intention to construct a cost effective set-up.

TEST RESULTS

There are several issues which have an affect upon the image accuracy. For example, the smoothness of the illuminating light affects the quality of the projection images and particularly disturbs the evaluation of the absolute level of radiation doses. In addition, the quality of the projection images is weakened by vignetting the lens and surrounding light and other imaging conditions.

In addition to the abovementioned projection image quality issues, tomography images are affected by the lens errors particularly with short focus lenses.

The distortions of tomography images were studied with pins (fig. 6). The pins were fixed on the gel basement in line so that the central pin hits on the rotation axis. The diameter of the pins is 0.6 mm and the spacing distances are 5 mm and 10 mm.

The pins were imaged using both Philips and Canon lenses. Figure 7 is a sinogram from the projection images taken with the Canon lens.

The tomography images were reconstructed from 200 and 400 projections using the Ram-Lak filter. The image quality of only 100 projections was not good enough for test purposes. The resulting tomography images show that the quality of the pin images weakens far from the rotating axis (see fig. 8). With the Canon lens, the pins are sharp up to 4 cm out from the rotating axis.

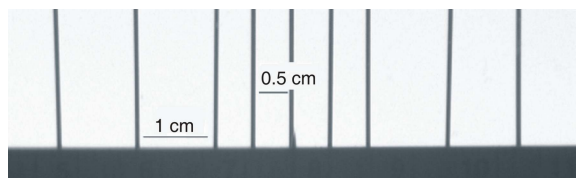


Figure 6. Test object built from pins on the gel basement

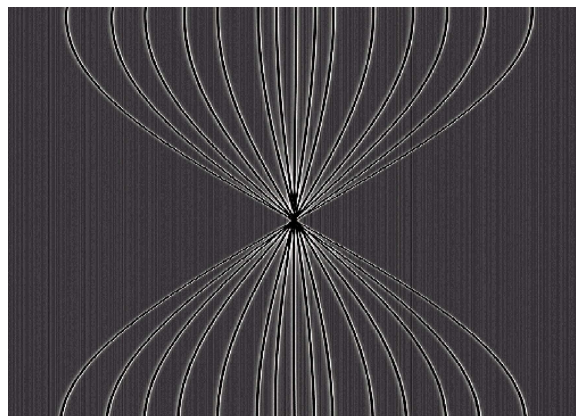


Figure 7. Sinogram which is calculated from the projection images taken with the Canon lens

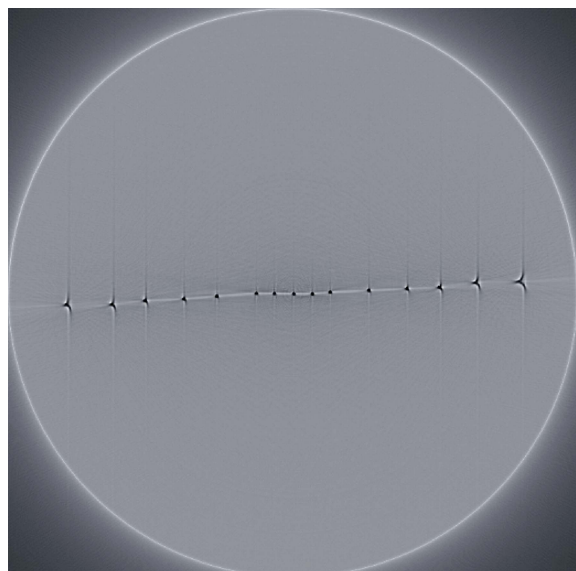


Figure 8. Tomography slice image of the test pins processed from the data taken with the Canon lens

The spreading of the pins can be seen more clearly with the short focus Philips lens (fig. 9). Only five central pin images are accurate.

In both cases (figs. 8 and 9), the accuracy of the pin images decreases when going far from the rotating axis. This experiment shows that the lens has remarkable effect on the image quality, particularly, far from the rotating axis.

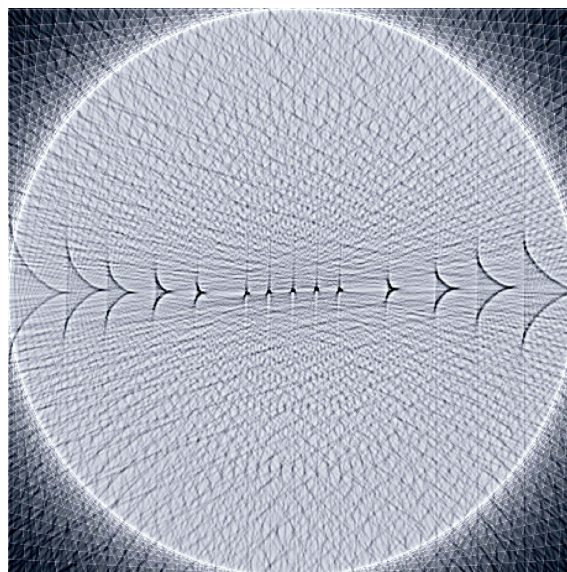


Figure 9. Tomography slice image of the test pins processed from the data taken with the Philips lens

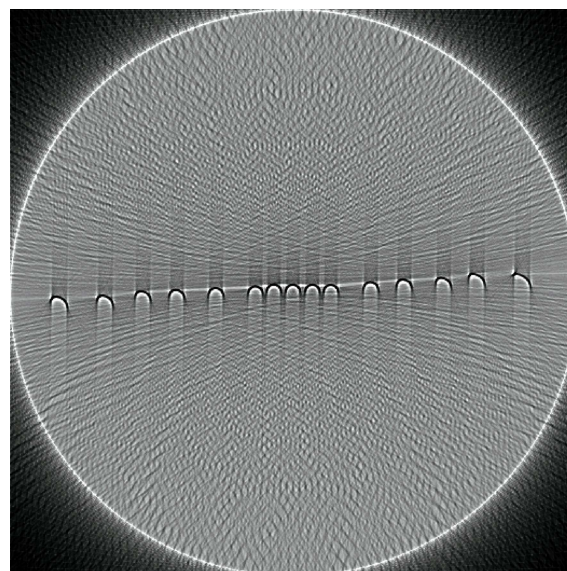


Figure 10. Tomography image of the pins when the camera is not pointed exactly on the rotating axis

When imaging pins, it is also possible to see that the image accuracy weakens when the camera is not pointed exactly on the rotating axis (fig. 10). The pins can be seen as the half circle images whose radius is equal to the error of the camera positioning. This error weakens image quality all across the imaging space.

A systematic inaccuracy of the imaging angle also creates an image distortion similar to the lens errors (fig. 11).

The optical density differences can be recognized in the gel if the local opacity gradient is large enough. For testing purposes, two square fields were radiated into the gel within each other so that the

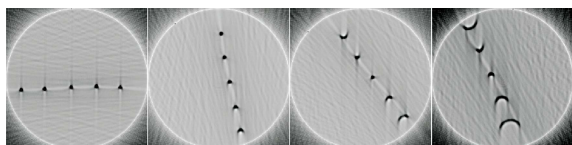


Figure 11. The tomography images of the pins, when the systematic error of the imaging angle is (from left) 0%, 1%, 5 %, and 10%

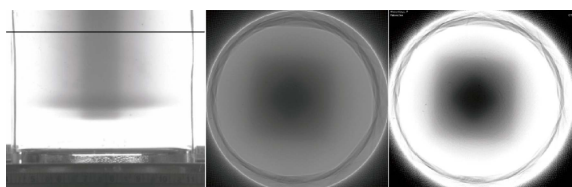


Figure 12. From left: Projection image of the gel with a slice plane marker, a tomography image on the slice plane and histogram smoothed tomography image

dose level of the inner field was 1.5 Gy and the outer 0.75 Gy. Figure 12 shows the results of the test. From the left, the first image shows a projection image with a slice plane marked with a black horizontal line. The next image shows the tomography image and the last one, the same image with a histogram process to emphasize the square fields. Notice that the square fields are at a 45 degree angle to each other. They can be distinguished, but the edges can not be seen clearly.

A dose response in gel dosimetry describes dependency between the radiation strength and the measured grayscale. Especially, when studying the absolute level of the radiation dose, the dependency must be linear, or at least mathematically deterministic. A linear dependency has been found, for example, in FSX gels (Ferrous Sulphate and Xylenol) [17], normoxic N-Vinylpyrrolidone based polymer gels (VIPET) [25]. Also an N-isopropyl acrylamide (NIPAM) polymer gel can be considered as a linear dependent [26].

In this study, the dose response of the MAGAT gel (Methacrylic Acid, Gelatine and Tetrakis phosphonium chloride) was studied by means of calibrating series of samples (fig. 13).

The gel samples (in fig. 13 from left to right) were radiated by the doses of 0, 15, 30, 80, 130, 150, 180, 200, 230, and 280 MU (monitor unit), where 1 Gy = 97.8 MU in the used radiation therapy unit. The median gray scale value was measured from the defined region of interest (ROI) of the tomography images of the samples. The defined ROI is equal in each sample and situated 15 mm from the bottom of the sample bottle by assuming that it is the place where the dose is at maximum. The tomography images of the slices can be seen in fig. 14 where an irradiated sample



Figure 13. Calibrating series made of MAGAT gel imaged after radiation. The opacity change due to growing radiation dose can easily be seen by eyes

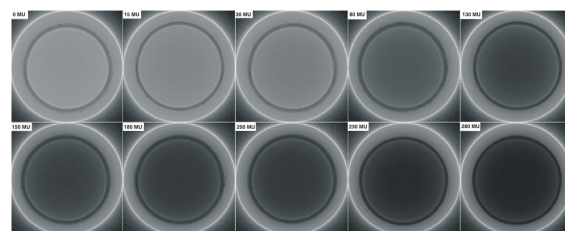


Figure 14. Tomography images of the ROI slices of MAGAT gel samples seen in fig. 13. The measured opacity values are used to evaluate the accuracy and linearity of the developed experimental installation

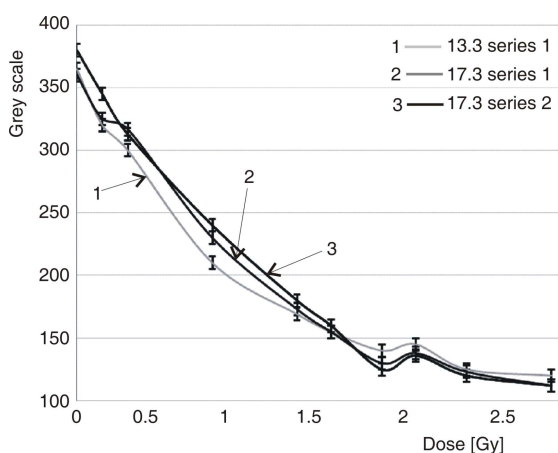


Figure 15. Experimental graph of the dose response of the MAGAT gel

is on the upper left, and a sample of 280 MU dose is on the lower right.

Two series of gel samples were prepared for studying dose responses, and they were measured on different days (13th and 17th of March). The results have been collected into fig. 15, where it can be seen that the measurements have managed to be repeated rather well. The slight difference might be explained by a continuing of the polymerization process between the imaging days. The unanticipated rise of the gray values of dose response at 2.04 Gy cannot be explained.

An important finding is that the MAGAT gel does not function linearly. The linearity, however, is not required if the dose response is systematic and can

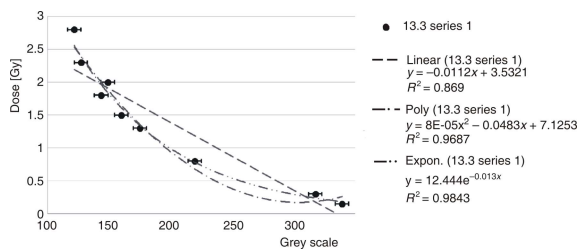


Figure 16. Matching of the dose response to the measured values of gray level

be matched [27]. A good approximation can be found by applying the exponential matching (fig. 16). The matching can still be improved by using the inverse values of gray level and polynomial matching, which leads to a correlation of $R^2 = 0.9885$ and thus to the acceptable accuracy for clinical use. Later, after acquiring enough experimental data, it is possible to develop automatic software for calibration.

DISCUSSION AND CONCLUSION

The developed optical tomography installation can be used to detect the opacity differences three-dimensionally. The imaging accuracy is close to the rotating axis less than 0.6 mm which is good enough for most radiation therapy applications. However, more studies and development work is needed to get the gel dosimetry, based on CCD camera technology, workable, accurate and reliable enough to replace the expensive and slow MRI based gel dosimetry.

The problems of using the optical computed tomography (optical-CT) based on the CCD camera have been studied and tried to be solved in many ways. For example, to get a better imaging accuracy, the so-called plano-convex lenses have been applied to solve the optical problems of the lens [17]. Also, a differential imaging used to differentiate the gel from its background in the projection images can be used to solve the problems of the refraction and the smoothness of the illuminating light source [22]. The problem of vignetting can be solved by using higher quality but more expensive lenses. Anyway, in this study, an accuracy better than 0.6 mm was achieved, close to the rotation axis.

In addition to the imaging accuracy, the repeatability of the measurement is important to consider for making it possible to also define the absolute doses from the gel samples. The MAGAT gel, which has been found successful with the MRI, has no linear dose response in optical-CT based dosimetry. The dose response of the FSX gel seems to be remarkably smoother. However, the FSX gel is much less sensitive than the MAGAT gel, and is therefore suitable when a wider dose scale is needed. In fact, a new gel with optimal optical parameters would be needed.

In conclusion, this study shows that the optical-CT is a promising gel dosimetry method for determining the dose distribution in radiation therapy. The studies should be continued to develop a reliable and accurate measuring method for quality control of this three-dimensional radiation therapy. This would lead to a more accurate and better managed radiation therapy in an easy, rapid and inexpensive form.

Defining dependency between the light source wavelength and the temperature emerges issues for further research. Also the iterative algorithms instead of the inverse radon transform should be considered to improve the quality of tomography images.

AUTHOR CONTRIBUTIONS

Measurement system build up, measurements and analyses were carried out by M. Kauppinen. Theoretical support was carried by E. Alasaarela, the manuscript was written by E. Alasaarela and M. Kauppinen. Gel samples preparation and radiation was carried out by S. Rouhiainen and tomography calculations and theoretical support was carried out by A. Koivula. All authors have analyzed and discussed the results.

REFERENCES

- [1] Webb, S., Intensity Modulated Radiation Therapy, Institute of Physics Publishing, Bodmin, GB., 2001, pp. 1-31
- [2] Gore, J. C., Kang, Y. S., Schulz, R. J., Measurement of Radiation Dose Distributions by Nuclear Magnetic Resonance Imaging, *Phys. Med. Biol.*, 29 (1984), 10, pp. 1189-1197
- [3] Mattila, S., Gel Dosimetry in the Verification of IMRT Treatment Planning, M. Sc. thesis (in Finnish) Department of Physical Sciences, University of Oulu, Oulu, Finland, 2005
- [4] Rouhiainen, S., Application of Gel Dosimetry, Ph. Lic. thesis (in Finnish) Department of Physical Sciences, University of Oulu, Oulu, Finland, 2010
- [5] Gustavsson, H., Radiotherapy Gel Dosimetry Development and Application of Normoxic Polymer Gels, Ph. D. Dissertation, Department of Medical Radiation Physics, Lund University, Malmö, 2004
- [6] Kak, A., Slaney, M., (2001) Principles of Computerized Tomographic Imaging, IEEE Press, New York, 1999, p. 327
- [7] Brinivasa, N., Rajgopal, K., Ramesh, B. R., An Algorithm for Computing the Discrete Radon Transform with Some Applications, Presented at the TENCON '89, the 4th IEEE Region 10 International Conference, Bombay, India, 1989
- [8] Arridge, S., Schweiger, M., Image Reconstruction in Optical Tomography, *Philosophical Transactions of the Royal Society B: Biological Sciences*, 352 (1997), 11, pp. 717-726
- [9] Pan, X., Tomographic Image Reconstruction, *American Association of Physicists in Medicine*, 41 (1999)
- [10] Boone, J. M., et al., The Essential Physics of Medical Imaging, Lippincott Williams & Wilkins, Philadelphia, 2002, p. 933
- [11] Young, H. D., Sears and Zemansky's University Physics, Pearson Addison-Wesley, San Francisco, Cal., USA, 2003, p. 1714

- [12] Kelly, R. G., Jordan, K. J., Battista, J. J., Optical CT Reconstruction of 3-D Dose Distributions Using the Ferrous-Benzoic-Xylenol (FBX) Gel Dosimeter, *Med. Phys.*, 25 (1998), 9, pp. 1741-1750
- [13] Krstajić, N., Doran, S. J., Fast Laser Scanning Optical-CT Apparatus for 3-D Radiation Dosimetry, *Phys. Med. Biol.*, 52 (2007), 11, pp. N257-NN63
- [14] Gore, J. C., Ranade, M., Maryanski, M. J., Radiation Dose Distributions in Three Dimensions from Tomographic Optical Density Scanning of Polymer Gels: 1. Development of an Optical Scanner, *Phys. Med. Biol.*, 41 (1996), 12, pp. 2695-2704
- [15] Oldham, M., et al., High Resolution Gel-Dosimetry by Optical-CT and MR Scanning, *Med. Phys.*, 28 (2001), 7, pp. 1436-1445
- [16] Krstajić, N., Doran, S. J., Focusing Optics of a Parallel Beam CCD Optical Tomography Apparatus for 3-D Radiation Gel Dosimetry, *Phys. Med. Biol.*, 51 (2006), 8, pp. 2055-2075
- [17] Wolodzko, J. G., Marsden, C., Appleby, A., CCD Imaging for Optical Tomography of Gel Radiation Dosimeters, *Med. Phys.*, 26 (1999), 11, pp. 2508-2513
- [18] Devakumar, D., Ravindran, P., Three-Dimensional Image Reconstruction for CCD Camera Based Optical Computed Tomography Scanner, *IEEE Nuclear Science Symposium Conference Record*, 4 (2007), M13-129, pp. 2965-2967
- [19] Jenneson, P. M., et al., Three-Dimensional Optical Tomography of Dose Distribution Using Radiation Sensitive Transparent Gels, *IEEE Nuclear Science Symposium Conference Record*, 1 (1999), N16-1, pp. 538-540
- [20] Doran, J. S., The History and Principles of Chemical Dosimetry for 3-D Radiation Fields: Gels, Polymers and Plastics, *Applied Radiation and Isotopes*, 67 (2008), 3, pp. 393-398
- [21] Krstajić, N., Doran, S., Characterization of a Parallel-Beam CCD Optical-CT Apparatus for 3-D Radiation Dosimetry, *Phys. Med. Biol.*, 52 (2007), 13, pp. 3693-3713
- [22] Brindha, S., Ravindran, B. P., Visalatchi, S., A simple Optical Cone Beam CT Set-Up for Gel "Readout", *Journal of Physics, Conference Series* 3, (2004), pp. 268-271
- [23] Ramachandran, G. N., Lakshminarayanan, A. V., Three Dimensional Reconstructions from radiographs and Electron Micrographs: Applications of Convolutions Instead of Fourier Transforms, *Proc. Natl. Acad. Sci.*, 68 (1971), 9, pp. 2236-2240
- [24] Shepp, L. A., Logan, B. F., The Fourier Reconstruction of Head Section, *IEEE Trans. Nucl. Sci.*, NS21 (1974), 3, pp. 21-43
- [25] Papadakis, A. E., A New Optical-CT Apparatus for 3-D Radiotherapy Dosimetry: Is Free Space Scanning Feasible?, *IEEE Trans. Med. Im.*, 29 (2010), 5, pp. 1204-1212
- [26] Hsieh, B.-T., Wu, J., Chang, Y.-J., Verification on the Dose Profile Variation of 3-D – NIPAM Polymer Gel Dosimeter, *IEEE Trans. Nucl. Science*, 60 (2013), 2, pp. 560-565
- [27] Ibbott, G. S., et al., Three-Dimensional Visualization and Measurement of Conformal Dose Distributions Using Magnetic Resonance Imaging of Bang Polymer Gel Dosimeters, *International Journal of Radiation Oncology Biology Physics*, 38 (1997), 5, pp. 1097-1103

Received on December 31, 2013

Accepted on June 27, 2014

Мати КАУПИНЕН, Еско АЛАСАРЕЛА, Антеро КОИВУЛА, Сини РОУХИАИНЕН

ПРИМЕНА ОПТИЧКЕ ТОМОГРАФИЈЕ ЗА МЕРЕЊЕ РАСПОДЕЛЕ ДОЗЕ У ТЕРАПИЈИ ЗРАЧЕЊЕМ

Дозиметрија се користи за потврду јачине дозе у вештачким узорцима (фантомима) пре давања планиране терапије пацијентима. Уобичајено, расподела дозе мери су у једној тачки или у више тачака једне равни. Нове технике у терапији зрачењем обезбеђују детаљније планирање расподеле дозе те постоји потреба за мерењем расподеле доза у три димензије. У ту сврху користе се гел дозиметри. Зрачење изазива промене у хемијском својству гела и мерењем тих хемијских промена одређује се расподела дозе зрачења. Конвенционална метода је употреба магнетне резонанце MRI, а као нова могућност јавља се оптичка компјутеризована томографија, оптичка-СТ. Оптичка-СТ је много практичнија и јефтинија у односу на MRI. У овом раду приказан је уређај направљен према методи оптичке-СТ заснован на употреби јефтиног материјала и једноставне реализације. Уређај користи CCD камере и флуоресцентне лампе. Резултати тестова показују да се ниво непрозирности озраченог гела може измерити са довољном тачношћу. Тачност је ограничена оптичком дисторзијом сочива, дисторзијом флуоресцентне лампе као извора светлости и шумом околине током мерења.

Кључне речи: гел дозиметар, мерење непрозирности, оптичка-СТ, томографија, терапија зрачењем